# *IMAGING WITH ENHANCED EARLY-TIME DIFFUSION SIGNAL*

*Elizabeth H. Bleszynski, Marek K. Bleszynski, and Thomas Jaroszewicz*
*Monopole Research, Thousand Oaks, CA 91360*

*Annual EM Contractors Review*
*Arlington, VA, January 09 –11, 2018*

*work sponsored by Air Force Office of Scientific Research*

*sparse media:* *mean-free path orders of magnitude larger than average separation between scatterers*

*examples:* *atmospheric clouds, fog, haze, dust, aerosols*

## ■ *objective*

- *investigate the problem of imaging and communication through sparse and discrete random media (such as atmospheric clouds, fog, dust, aerosols, …) with optical/near-infrared pulsed signals in the framework of radiative transport equation (RTE)*

## ■ *previous work*

- *we presented theoretical analysis indicating that for a short infrared/optical pulse propagating in a sparse medium composed of scatterers large compared to the wavelength, there exists, in the time-resolved intensity, an early-time diffusion component which,*

  - *immediately follows the coherent signal*

  - *is attenuated proportionally to the non-diffractive cross-section on an average medium constituent (i.e. significantly weaker than the coherent component whose attenuation is governed by the total cross-section)*

  - *can be extracted by high-pass filtering (no time-gating required)*

■ *example: time-resolved intensity for two penetration depths, 72 m and 94 m, in an atmospheric cloud (for an omnidirectional source) **

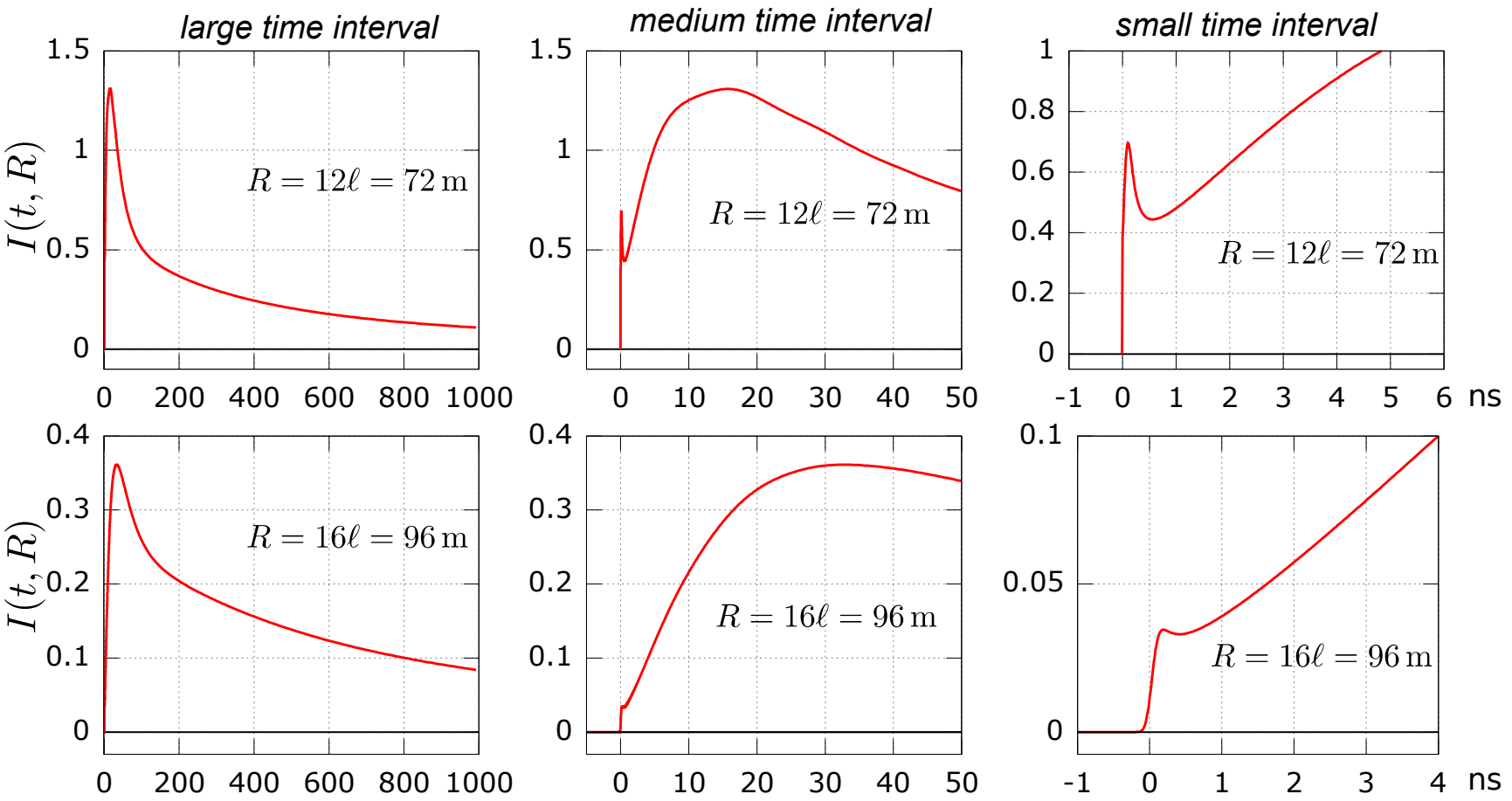


- *time-resolved intensity exhibits a sharply rising narrow peak at an early time*
- *as the propagation distance increases, the the early-time diffusion signal starts to overlap with the late-time diffusion but its sharply rising edge remains*

* *E. Bleszynski, M. Bleszynski, and T. Jaroszewicz, "Early-time diffusion in pulse propagation through dilute random media", Optics Letters, v. 39, pp. 5862-5865, 2014*

## ■ *characteristic features of the early-time diffusion signal*

*intensity of a propagating pulse in addition to the ballistic contribution and a wide, late-time diffusive tail exhibits a narrow early-time diffusive component characterized by:*

- *significantly reduced attenuation in comparison to the ballistic component*

  *attenuation factors:* *early-time diffusion* $\sim \mathrm{e}^{-n_0\,\sigma_{\text{non-diffr}}\,R}$
  *ballistic* $\sim \mathrm{e}^{-n_0\,\sigma_{\text{tot}}\,R}$ $\qquad \sigma_{\text{non-diffr}} \approx 0.65\,\sigma_{\text{tot}}$

- *sharp rise hence rich high frequency content → possibility of extraction from the received signal by filtering - no time gating required*

*propagation distance in atmospheric cloud ~100* m

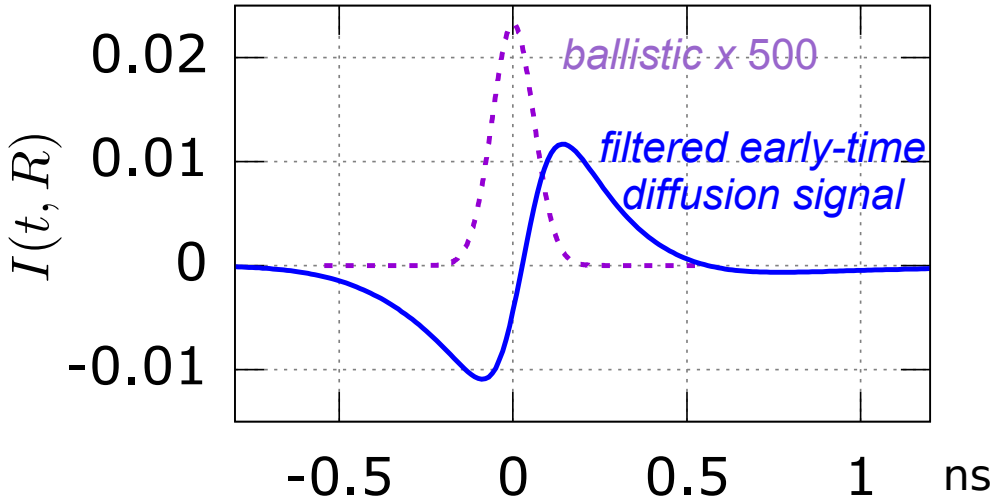

## ■ *parameters and characteristic length scales*

### ► *medium – atmospheric cloud*

| | | |
|---|---|---|
| *scatterers* | *water droplets with gamma radius distribution* | |
| *average scatterer radius* | $a \simeq 5\mu\mathrm{m}$ | |
| *number density* | $n_0 = 10^9\,\mathrm{m}^{-3}$ | |
| *average scatterer-scatterer distance* | $d \simeq 1\,\mathrm{mm}$ | *or more* |
| *resultant mean free path* | $\ell_\mathrm{t} = d^3/\sigma_\mathrm{t} \simeq 6\,\mathrm{m}$ | *or more* |

*(where $\sigma_\mathrm{t}$ is the total scattering cross-section on an average medium scatterer computed from Mie solution)*

### ► *transmitted pulse parameters*

| | | |
|---|---|---|
| *pulse carrier wavelength* | $\lambda_0 \lesssim 1\,\mu\mathrm{m}$ | |
| *e.g.* | $\lambda_0 = 0.633\,\mu\mathrm{m}$ | *(red light)* |
| | $\lambda_0 = 0.385\,\mu\mathrm{m}$ | *(near UV)* |
| *pulse duration of interest* | $T_\mathrm{p} \simeq 0.1\,\mathrm{ns}\,, \quad cT_\mathrm{p} \simeq 3\,\mathrm{cm}$ | |

*pulse should not extend past the duration of the early-time diffusion (ETD) enhancement*

## ■ *parameters and characteristic length scales*

### ▶ *early-time diffusion (ETD) scales*

*typical parameters:*

$$a = 5\mu\mathrm{m} \qquad k_0\, a = \frac{2\pi}{\lambda_0} a \approx 50 \qquad \ell_\mathrm{t} = 6\,\mathrm{m} \qquad \frac{R}{\ell_\mathrm{t}} = 20$$

*characteristic ETD rise time:*

$$\Delta t_\mathrm{ETD} \approx \frac{0.1}{(k_0 a)^2} \frac{R^2}{v_0\, \ell_\mathrm{t}} \qquad \Delta t_\mathrm{ETD} \approx 0.3\,\mathrm{ns}$$

*angular width of the ETD enhancement* $\approx$ *angular width of the diffractive peak of the differential cross section*

$$\Delta\theta_\mathrm{ETD} \approx \frac{1}{k_0 a} \qquad \Delta\theta_\mathrm{ETD} \approx 0.02\,\mathrm{rad}$$

### ▶ *late-time diffusion (LTD) scales*

*for comparison: ordinary late-time diffusion scale*

$$\Delta t_\mathrm{LTD} \sim \frac{\ell_\mathrm{t}}{v_0} \approx 20\,\mathrm{ns}$$

## ■ *parameters and characteristic length scales*

### ► *relation between pulse time scales and motion of the atmosphere*

*laminar and turbulent motion of the atmosphere constantly changes configuration of the medium*

*- consider gentle breeze (3 Beaufort) – air velocity* $v \lesssim 5\,\mathrm{m/s}$

*- medium configuration can be considered frozen during the time interval medium constituents move by less than a wavelength, i.e., during* $\Delta t = \lambda_0 / v \approx 100\,\mathrm{ns}$

*therefore,*

*- medium can be considered frozen during the ETD signal time* $\Delta t_{\mathrm{ETD}} \approx 0.3\,\mathrm{ns}$ *(during this time droplets are displaced by* $\Delta r = v\,\Delta t_{\mathrm{ETD}} \lesssim 2.5\,\mathrm{nm}$ *)*

*- ~ 100 pulses can be transmitted to generate one short exposure image before medium changes appreciably (to capture more photons to improve signal to noise ratio)*

*(RTE models an ensemble average of intensities for various medium configurations and not intensity for a single pulse, therefore an ensemble average of pulse intensities should be used when performing an imaging procedure)*

## ■ physical origin of the early-time diffusion phenomenon

- *differential cross section on a single water droplet exhibits a sharp forward peak and a flat large-angle tail when the scatterer is large compared to the wavelength,* $a >> \lambda_0$

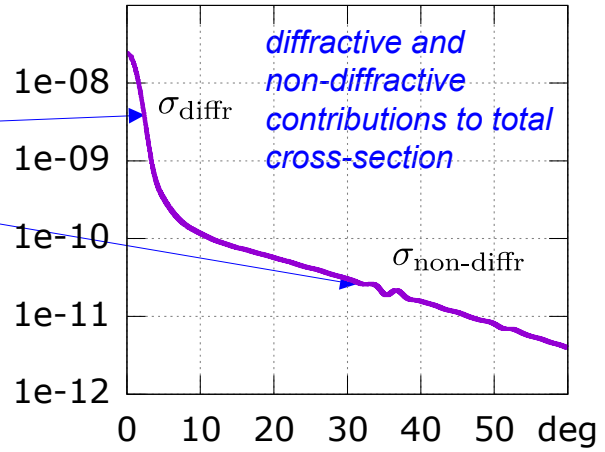


- *this "two slope" behavior leads to two scattering mechanisms in the medium:*

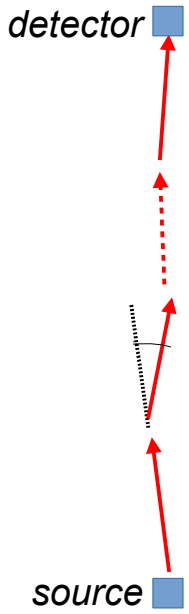


*a sequence of small angle diffractive scatterings*

*persistent random walk (small changes in direction):*

*few scatterings* → *short total travel path* → *small time delay* → *early-time diffusion*

*non-diffractive large-angle scattering*

*ordinary random walk (arbitrary changes in direction):*

*many scatterings* → *long total travel path* → *long time delay* → *late-time diffusion*

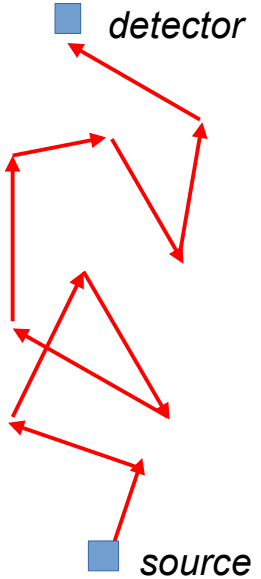

## Radiative Transport Equation (RTE)

- *rigorous description of radiance propagation in random, discrete scatterer medium can be obtained through Bethe-Salpeter (B-S) equation (practically intractable)*

- *assumptions of sparse, stationary, statistically homogeneous medium allow to reduce Bethe-Salpeter equation to RTE describing propagation of radiance as a function time, space-point, and energy flux direction*

*integro-differential form of RTE:*

$$\left(\mu_{\mathrm{t}} + \frac{1}{v_0}\,\partial_t + \hat{\boldsymbol{s}}\cdot\boldsymbol{\nabla}_{\boldsymbol{R}}\right) I(t,\boldsymbol{R};\hat{\boldsymbol{s}}) - \int \mathrm{d}^2\hat{s}'\;\widetilde{\Sigma}(\hat{\boldsymbol{s}}\cdot\hat{\boldsymbol{s}}')\, I(t,\boldsymbol{R};\hat{\boldsymbol{s}}') = S(t)\,\delta^3(\boldsymbol{R})$$

*coherent propagation with exponential attenuation*

*incoherent scattering*

*the quantities involved:*

$I(t,\boldsymbol{R};\hat{\boldsymbol{s}})$ - *radiance (time- and angle-resolved intensity) generated by an omnidirectionally radiated pulse located at the origin,* $\boldsymbol{R}=\boldsymbol{0}$

$\mu_{\mathrm{t}} = n_0\,\sigma_{\mathrm{t}}$ - *coherent wave attenuation coef*

$\widetilde{\Sigma}(x) = n_0\,\sigma(x)$ - *scattering kernel*

$n_0$ - *number density*

$\sigma_{\mathrm{t}}$ - *ensemble-averaged total cross-section on a medium constituent*

$\sigma(x)$ - *ensemble-averaged differential cross-section on a medium constituent*

*note: in imaging applications described below scattering from the scene is mostly diffuse and can be described in terms of omnidirectional sources*

▶ expand $I(t;\boldsymbol{R},\hat{\boldsymbol{s}})$

- in plane waves in the variables t and $\boldsymbol{R}$ : $\mathrm{e}^{-\mathrm{i}\,\Omega\,t}\,\mathrm{e}^{\mathrm{i}\,\boldsymbol{P}\cdot\boldsymbol{R}}$
- in (rotated) spherical harmonics in the variable $\hat{\boldsymbol{s}}$ : $\mathrm{Y}_{l,m}(\hat{\boldsymbol{s}};\hat{\boldsymbol{P}})$

$$I(t,\boldsymbol{R};\hat{\boldsymbol{s}}) = \int\frac{\mathrm{d}\Omega}{2\pi}\int\frac{\mathrm{d}^3P}{(2\pi)^3}\,\mathrm{e}^{-\mathrm{i}\,\Omega\,t}\,\mathrm{e}^{\mathrm{i}\,\boldsymbol{P}\cdot\boldsymbol{R}}\,\widetilde{I}(\Omega,\boldsymbol{P};\hat{\boldsymbol{s}})$$

$$= \int\frac{\mathrm{d}\Omega}{2\pi}\int\frac{\mathrm{d}^3P}{(2\pi)^3}\sum_{l=0}^{\infty}\sum_{m=-l}^{l} I_l^m(\Omega,P)\,\mathrm{e}^{-\mathrm{i}\,\Omega\,t}\,\mathrm{e}^{\mathrm{i}\,\boldsymbol{P}\cdot\boldsymbol{R}}\,\mathrm{Y}_{l,m}(\hat{\boldsymbol{s}};\hat{\boldsymbol{P}})$$

▶ substitute the radiance into RTE, truncate the expansion in $l$

→ obtain a set of matrix equation (one for each $m$ for the vectors $I^m(\Omega,P)$ consisting of coefficients $I_l^m(\Omega,P)$

$$\sum_{l'}\left(-\mathrm{i}\,\frac{\Omega}{v_0}\,\mathrm{I} + M^m(P)\right)_{l,l'} I_{l'}^m(\Omega,P) = \widetilde{S}(\Omega)\,\delta_{m,0}\,\delta_{l,0}$$

▶ diagonalize $M^m(P)$

frequency eigenvalue ↙

$$M^m(P)\,w_j^m(P) = \mathrm{i}\,\frac{\Omega_j^m(P)}{v_0}\,w_j^m(P)$$ ← eigenvector

▶ radiance = resolvent of $M^m(P)$

$$I_l^m(\Omega,P) = \mathrm{i}\,v_0\,\delta_{m,0}\sum_j \frac{w_{j,\,l}^0(P)\,w_{j,\,0}^0(P)}{\Omega-\Omega_j^0(P)}\,\widetilde{S}(\Omega)$$

## solving RTE for the radiance

- *supporting notes (explicit expression for $M^m(P)$ )*

$$\int \mathrm{d}^2\hat{s}\ \mathrm{Y}^*_{l,m}(\hat{\boldsymbol{s}};\hat{\boldsymbol{P}})\ \mathrm{i}\,\boldsymbol{P}\cdot\hat{\boldsymbol{s}}\ \mathrm{Y}_{l',m}(\hat{\boldsymbol{s}};\hat{\boldsymbol{P}}) = \mathrm{i}\,P\left(\delta_{l,\,l'+1}\,b^m_l + \delta_{l',\,l+1}\,b^m_{l'}\right)$$

$$\int \mathrm{d}^2\hat{s} \int \mathrm{d}^2\hat{s}'\ \mathrm{Y}^*_{l,m}(\hat{\boldsymbol{s}};\hat{\boldsymbol{P}})\ \Sigma(\hat{\boldsymbol{s}}\cdot\hat{\boldsymbol{s}}')\,\mathrm{Y}_{l',m}(\hat{\boldsymbol{s}}';\hat{\boldsymbol{P}}) = \delta_{l,\,l'}\,\Sigma_l$$

$$b^m_l = \sqrt{\frac{l^2-m^2}{4l^2-1}} \qquad\qquad \Sigma_l = 2\pi \int_{-1}^{1} \mathrm{d}x\,\Sigma(x)\,\mathrm{P}_l(x)$$

$$\sum_{l'}\Bigg[-\mathrm{i}\,\frac{\Omega}{v_0}\,\delta_{l,\,l'} + \underbrace{\left(\mu_\mathrm{t}-\Sigma_l\right)\delta_{l,\,l'} + \mathrm{i}\,P\left(\delta_{l,\,l'+1}\,b^m_l + \delta_{l',\,l+1}\,b^m_{l'}\right)}_{M^m_{l,l'}(P)}\Bigg] I^m_{l'}(\Omega,P) = \delta_{m,0}\,\delta_{l,0}\,\widetilde{S}(\Omega) \qquad \text{for all}\ \ m,l$$

## solving RTE for the radiance

- substitute $I_l^m(\Omega, P)$ into the expression for the radiance

$$I(t,\boldsymbol{R};\hat{\boldsymbol{s}}) = \int\frac{\mathrm{d}\Omega}{2\pi}\int\frac{\mathrm{d}^3P}{(2\pi)^3}\,\mathrm{e}^{-\mathrm{i}\,\Omega\,t}\,\mathrm{e}^{\mathrm{i}\,\boldsymbol{P}\cdot\boldsymbol{R}}\,\widetilde{I}(\Omega,\boldsymbol{P};\hat{\boldsymbol{s}})$$

$$= \int\frac{\mathrm{d}\Omega}{2\pi}\int\frac{\mathrm{d}^3P}{(2\pi)^3}\,\mathrm{e}^{-\mathrm{i}\,\Omega\,t}\,\mathrm{e}^{\mathrm{i}\,\boldsymbol{P}\cdot\boldsymbol{R}}\sum_{l=0}^{\infty}\mathrm{i}\,v_0\sum_j\frac{w_{j,l}^0(P)\,w_{j,0}^0(P)}{\Omega-\Omega_j^0(P)}\,\mathrm{Y}_{l,0}(\hat{\boldsymbol{s}};\hat{\boldsymbol{P}})\;\widetilde{S}(\Omega)$$

$$= v_0\,\mathrm{H}(t)\sum_j\int\frac{\mathrm{d}^3P}{(2\pi)^3}\;\underbrace{\mathrm{e}^{-\mathrm{i}\,\Omega_j^0(P)\,t}\,\mathrm{e}^{\mathrm{i}\,\boldsymbol{P}\cdot\boldsymbol{R}}\sum_l w_{j,l}^0(P)\,\mathrm{Y}_{l,0}(\hat{\boldsymbol{s}};\hat{\boldsymbol{P}})}_{\Psi_{j,\boldsymbol{P}}^0(t,\boldsymbol{R},\hat{\boldsymbol{s}})}\;\underbrace{w_{j,0}^0(P)}\;\;\widetilde{S}(\Omega)$$

$$\frac{1}{\sqrt{4\pi}}\int\mathrm{d}^2\hat{s}'\;\Psi_{j,\boldsymbol{P}}^0(0,\boldsymbol{0},\hat{\boldsymbol{s}}')$$

*eigenfunctions*

*integrated over initial flux direction, because the source is omnidirectional*

## solving RTE for the radiance

- substitute $I_l^0(\Omega, P)$ into the expression for the radiance

$$I(t, \boldsymbol{R}; \hat{\boldsymbol{s}}) = \frac{v_0}{\sqrt{4\pi}} \int_{-\infty}^{t} \mathrm{d}t' \sum_j \int \frac{\mathrm{d}^3 P}{(2\pi)^3} \, \mathrm{e}^{-\mathrm{i}\,\Omega_j^0(P)\,(t-t')} \, \Psi_{j,\boldsymbol{P}}^0(\boldsymbol{R}, \hat{\boldsymbol{s}}) \int \mathrm{d}^2\hat{\boldsymbol{s}}' \, \Psi_{j,\boldsymbol{P}}^0(\boldsymbol{0}, \hat{\boldsymbol{s}}') \, S(t')$$

where

$$\Psi_{j,\boldsymbol{P}}^m(t, \boldsymbol{R}, \hat{\boldsymbol{s}}) = \mathrm{e}^{-\mathrm{i}\,\Omega_j^m(P)\,t} \, \mathrm{e}^{\mathrm{i}\,\boldsymbol{P}\cdot\boldsymbol{R}} \sum_l w_{j,l}^m(P) \, \mathrm{Y}_{l,m}(\hat{\boldsymbol{s}}; \hat{\boldsymbol{P}})$$

each $\Psi_{j,\boldsymbol{P}}^m$ represents a radiance configuration mode propagating as a plane wave with the (real) wave number $\boldsymbol{P}$ and the (complex) frequency $\Omega_j^m(P)$;
its dependence on the flux direction $\hat{\boldsymbol{s}}$ is given by a combination of spherical harmonics and remains independent of time and spatial coordinates

- interpretation of $\mathrm{Im}\,\Omega_j^m(P)$ and $\mathrm{Re}\,\Omega_j^m(P)$

$$\mu_j^m(P) \equiv -\frac{\mathrm{Im}\,\Omega_j^m(P)}{v_0} \geq 0$$

P-dependent attenuation coefficient for the j-th mode

$$-v_0 \leq v_j^m(P) \equiv \frac{\mathrm{Re}\,\Omega_j^m(P)}{P} \leq v_0$$

radiance propagation velocity of the j-th mode

$\Omega_j^m(P)$ form "trajectories" of eigenvalues moving on the complex $\Omega$ plane

## some relevant features of frequency eigenvalues and eigenvectors of RTE

### real and imaginary parts of frequency eigenvalues as a function of P

$\frac{\mathrm{Re}\,\Omega_j^0(P)}{P}$ = radiance propagation velocity of $j$-th mode

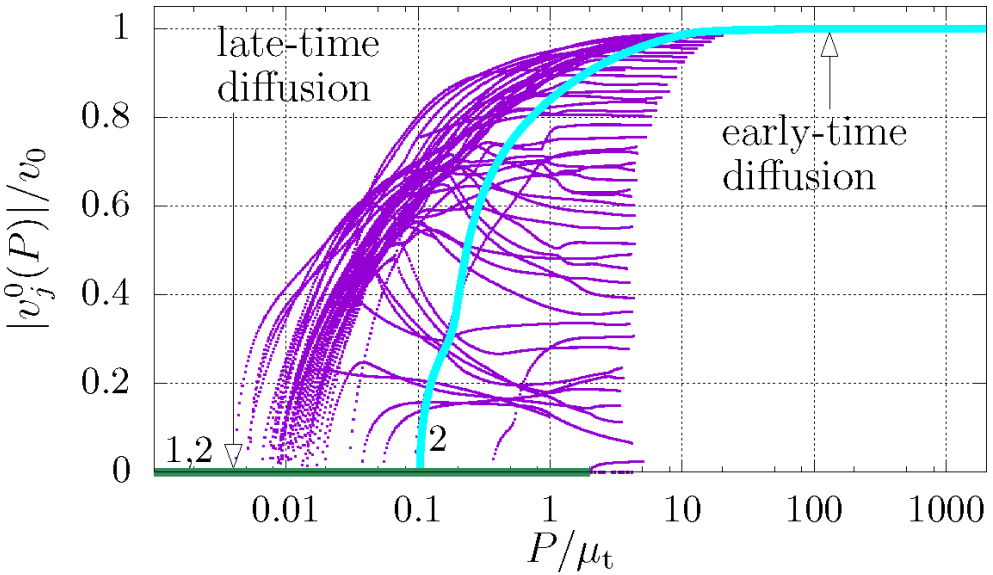


- velocities of only discrete modes plotted
- velocity trajectories terminated for values at which attenuation reaches that of the coherent wave

$\frac{\mathrm{Im}\,\Omega_j^0(P)}{v_0}$ = $j$-th mode attenuation coefficient

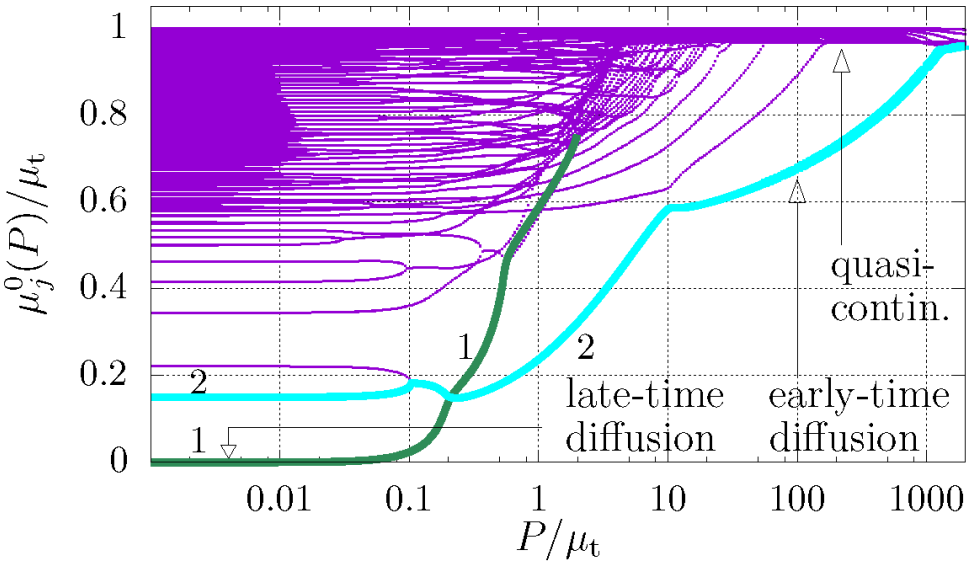


- attenuation coefficients for all the modes (including those belonging to "quasi-continuum")

- at distances small compared to the mean-free path ( $R \lesssim 10\,\ell_t$ ) all modes are important
- at large distances intensity is dominated by a few dominant (least attenuated) modes (marked with thick lines and numbered 1 – 4)
- for $P/\mu_t < 0.1$ the dominant trajectories are characterized by zero-velocity and their associated eigenmodes have flat, omnidirectional distribution => they represent the ordinary, late-time diffusion
- for $P/\mu_t \approx 1$ trajectory "2" nearly reaches coherent speed velocity and its associated eigenmode attains narrow angular distribution => clear indication of early-time diffusion

## *some relevant features of frequency eigenvalues and eigenvectors of RTE*

- *angular distribution of leading (least attenuated) RTE modes for different values of P*

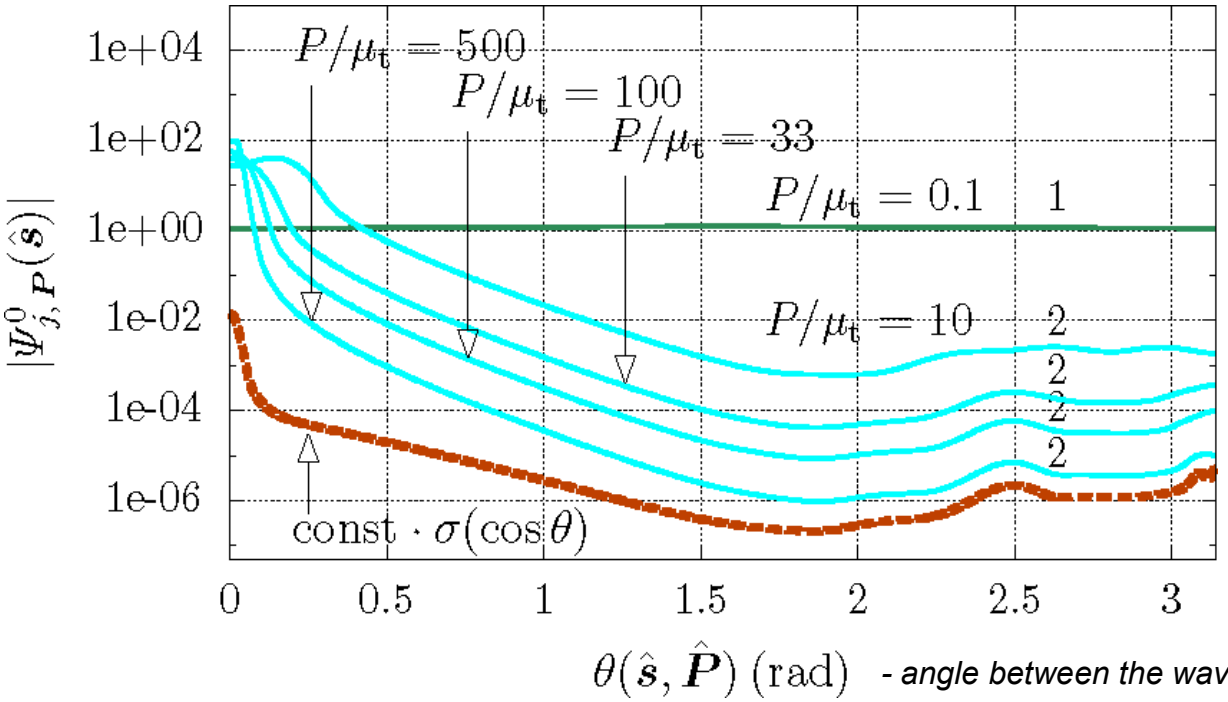


*- angle between the wave vector **P** and the flux direction*

*for small P the dominant eigenmodes have nearly flat angular distribution*

*for high P angular distributions of the dominant eigenmodes are at least as narrow as that of the cross-section*

## *filtered and unfiltered time-resolved intensities for beams of various widths*

*penetration depth ~100m*

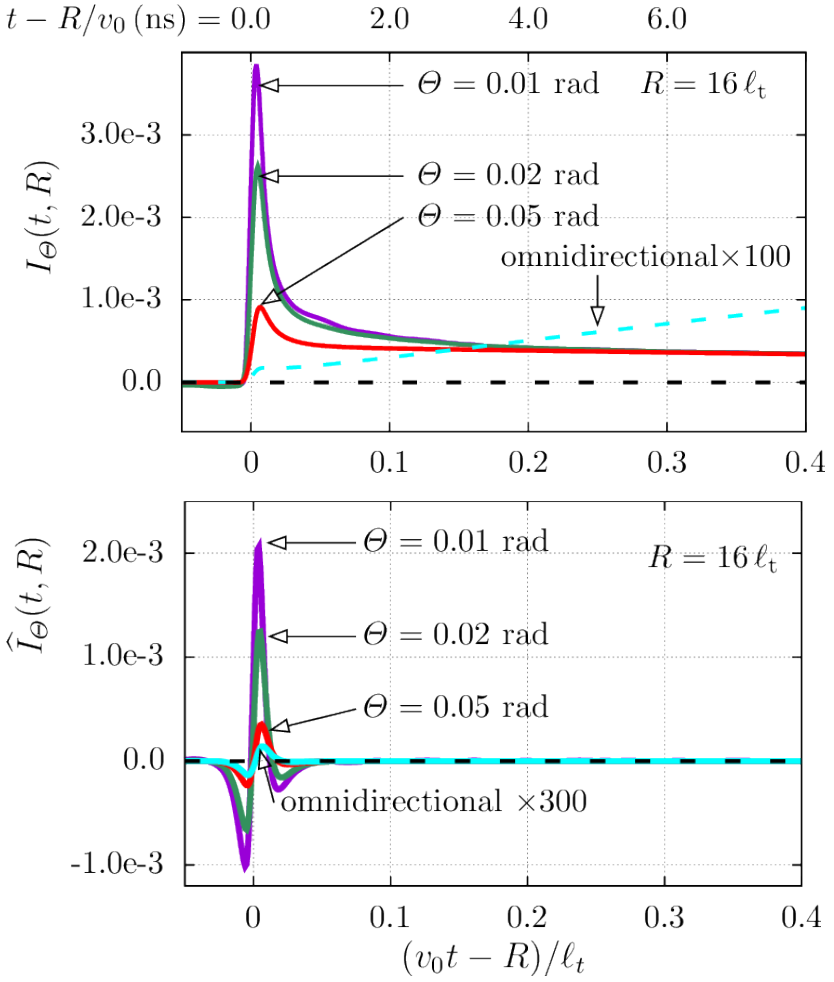


*penetration depth ~150m*

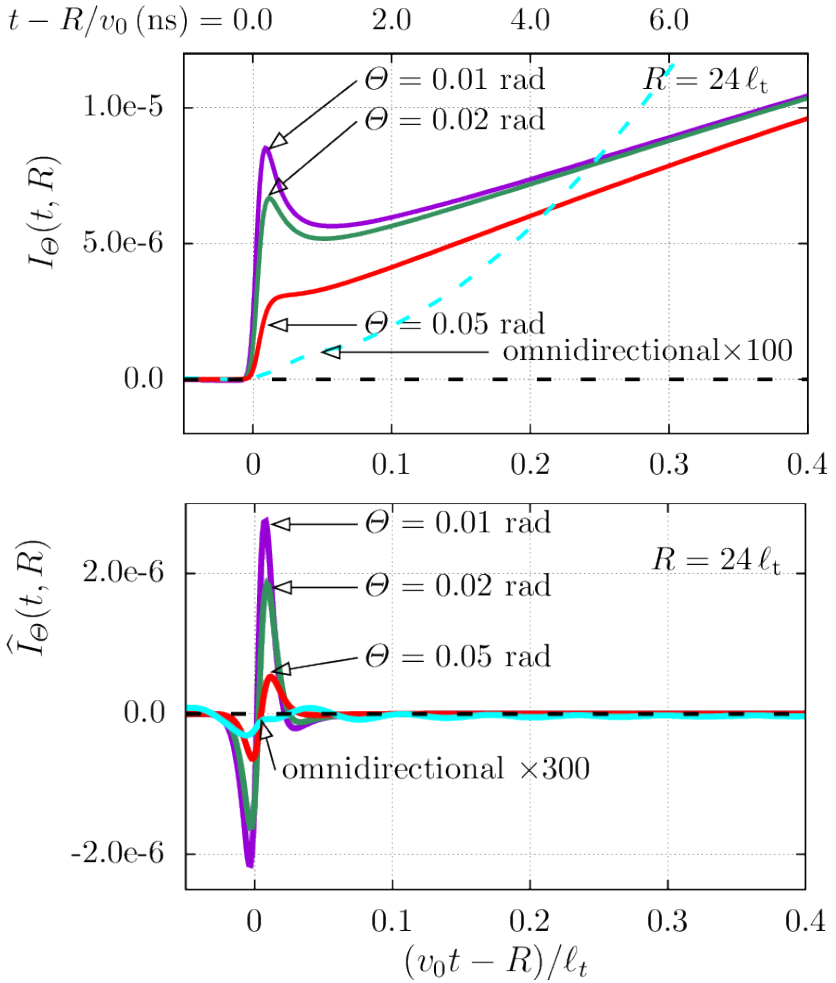


*received time-resolved intensities*

*filtered time-resolved intensities*

*note: we observe enhancement of the early-time wrt the late-time diffusion component with the decreasing width of the beam*

- *we investigated modal decomposition of RTE and identified dominant propagation modes responsible for early- and late-time diffusion*

- *we studied sources radiating with arbitrary angular distributions*

- *we showed that modulation of the source angular distribution may lead to strengthening of the early-time diffusion effect*

*can these findings be applied in communication and imaging scenarios?*

- *using early-time diffusion signal in communication*

  - *short rise time of the received signal allows high transfer rates*

## *using early-time diffusion signal in imaging*

- *assume a non-scanning imaging scenario*

  *- array of sensors = array of pixels (with possibly in-pixel processing)*

  *- image calibrated in angles:* $\varrho = \theta$

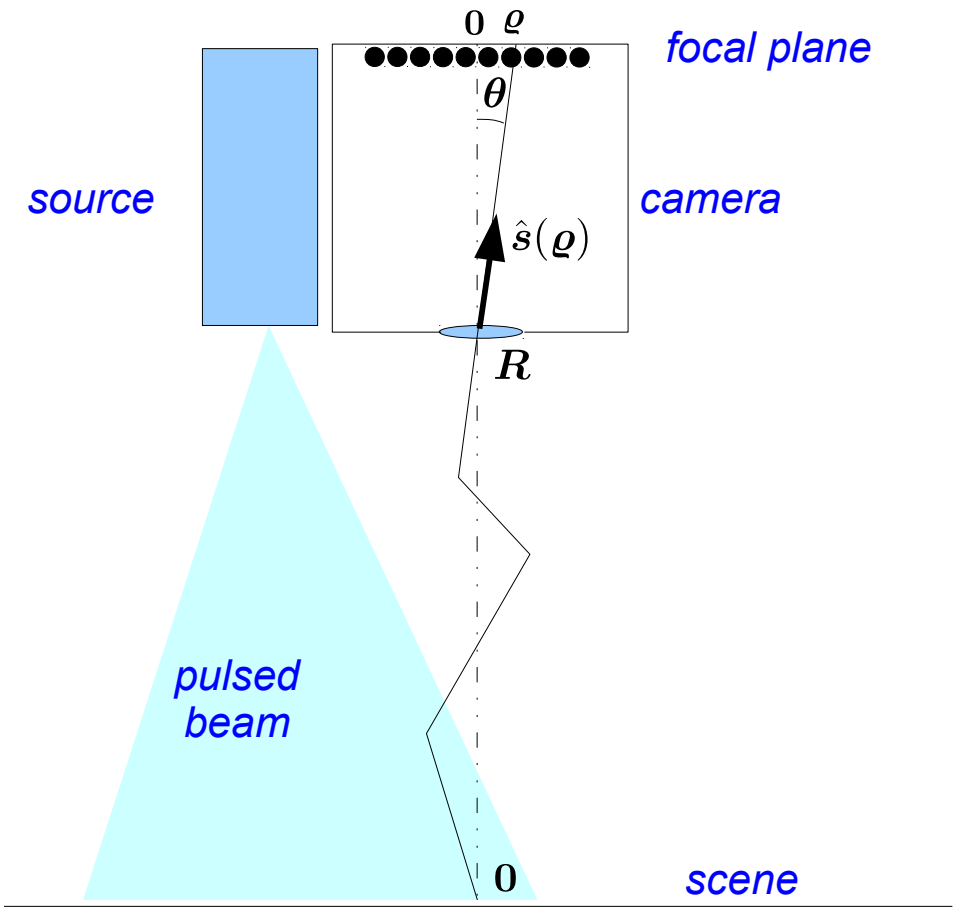


*reflecting point on the illuminated scene at the point* $\mathbf{0}$
*– approximately omnidirectional radiation*

## ■ *using early-time diffusion signal in imaging*

### ► *image formation procedure (schematically):*

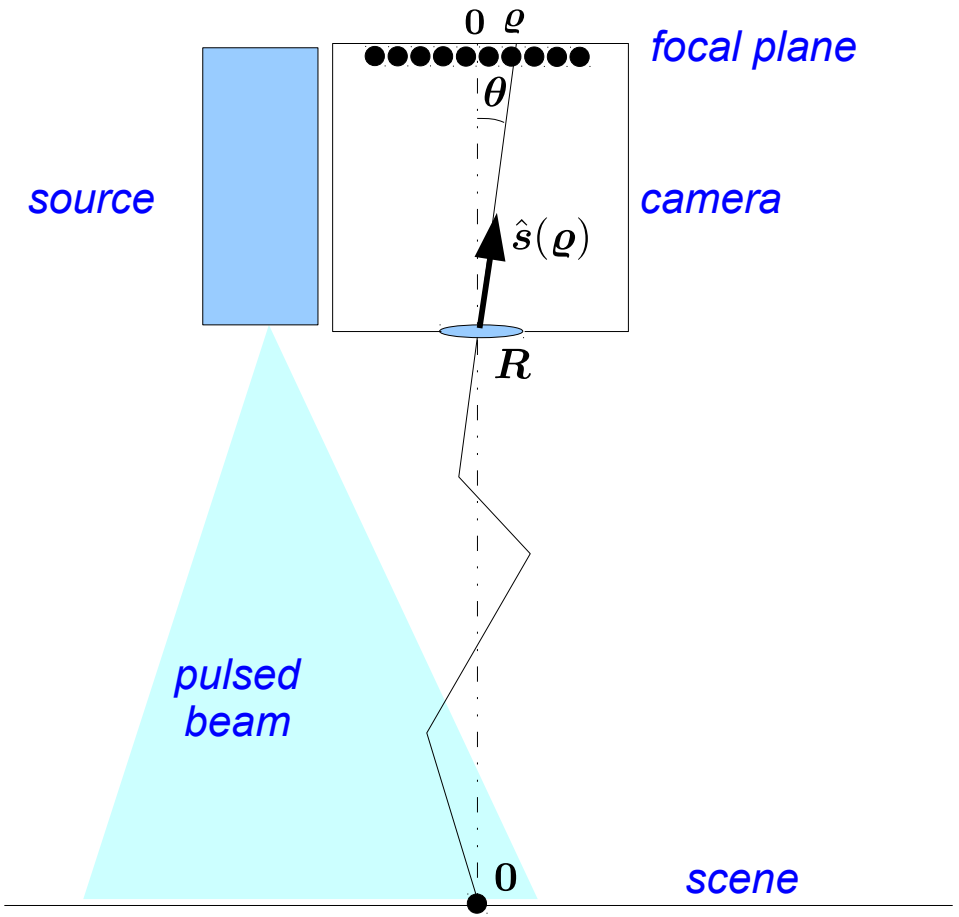


*reflecting point on the illuminated scene at the point* $\mathbf{0}$
*– approximately omnidirectional radiation*

*- for each transmitted/received pulse, each sensor located at* $\varrho = \theta$ *registers intensity observed at the camera location* $\boldsymbol{R}$ *arriving in the direction* $\hat{\boldsymbol{s}}(\varrho)$

*- intensity, i.e., radiance* $I(t, \boldsymbol{R}; \hat{\boldsymbol{s}}(\varrho))$*, is time-dependent and contains a large diffusive component*

*- for each pixel we process intensity by*

- *filtering in time to extract the early-time diffusive component*
- *integrating absolute value of the signal*
- *storing the result as the image intensity at that pixel*

*hence, the point-spread function (PSF), i.e., image of a point object, is related to radiance by*

$$\Lambda(R, \varrho) = \int_{t_1}^{t_2} \mathrm{d}t \left| \int \mathrm{d}t' \, \Phi(t - t') \, I(t', \boldsymbol{R}; \hat{\boldsymbol{s}}(\varrho)) \right|$$

*high-pass filter*

*integration interval capturing the ETD signal*

## using early-time diffusion signal in imaging

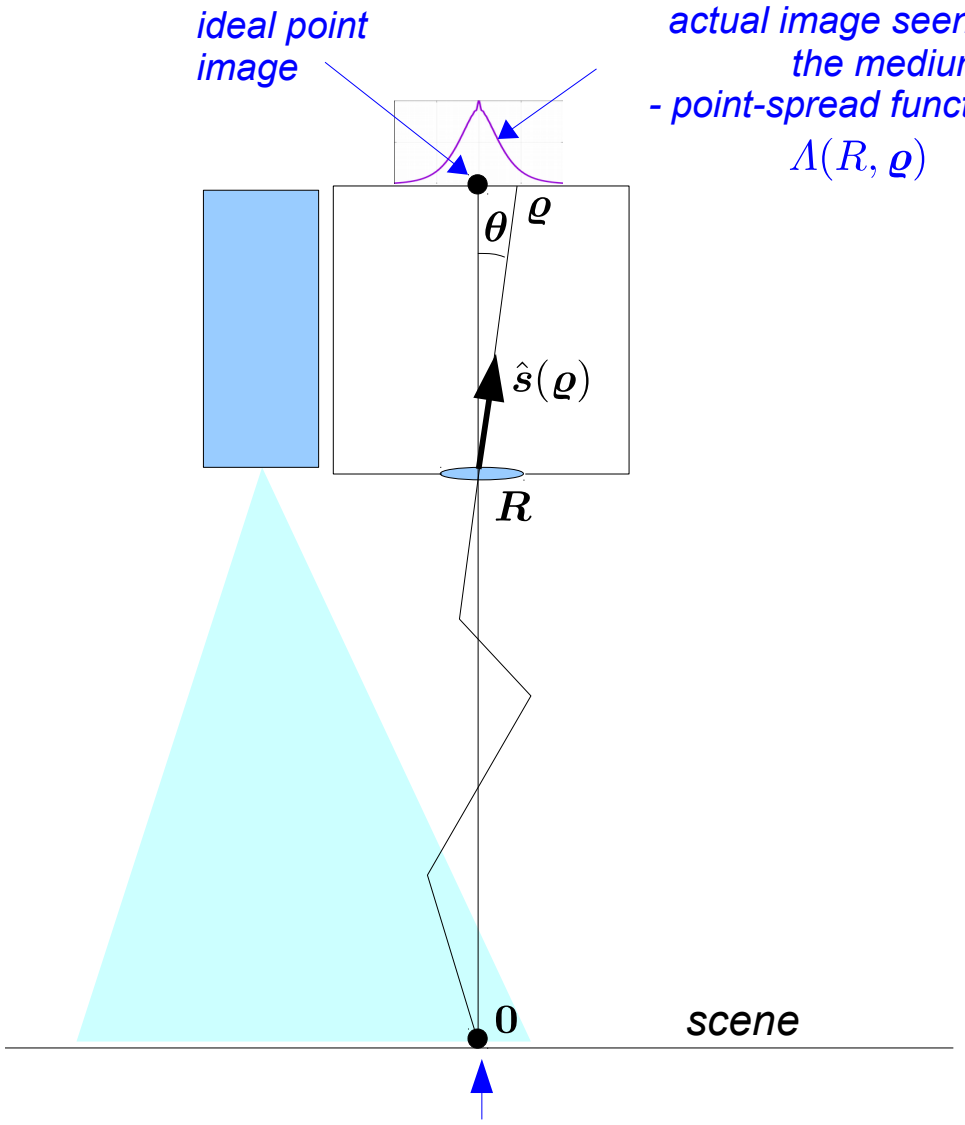


reflecting point on the illuminated scene at the point $\mathbf{0}$
– approximately omnidirectional radiation

- point-spread function (PSF)
  - image of a point object

$$\Lambda(R, \boldsymbol{\varrho})$$

- modulation-transfer function (MTF)
  - Fourier (Hankel) transform

$$\widetilde{\Lambda}(R, \boldsymbol{q}) = \int \mathrm{d}^2\varrho \; \mathrm{e}^{-\mathrm{i}\,\boldsymbol{q}\cdot\boldsymbol{\varrho}}\, \Lambda(R, \boldsymbol{\varrho})$$

- convolution of the PSF $\Lambda$ with the ideal image $f \;\rightarrow$ blurred image

$$F(R, \boldsymbol{\varrho}) = \int \mathrm{d}\varrho' \Lambda(R, \boldsymbol{\varrho} - \boldsymbol{\varrho}')\, f(\boldsymbol{\varrho}')$$

- reconstruction of the ideal image from the blurred image

$$\widetilde{F}(R, \boldsymbol{q}) = \widetilde{\Lambda}(R, \boldsymbol{q})\, \widetilde{f}(\boldsymbol{q})$$

$$\widetilde{f}(\boldsymbol{q}) = \widetilde{F}(R, \boldsymbol{q}) / \widetilde{\Lambda}(R, \boldsymbol{q})$$

- usually an ill-conditioned inverse problem, also $F(R, \boldsymbol{q})$ not known exactly (noise)

## point spread function (PSF) and modulation transfer function (MTF) evaluation scheme

- recall: point spread function: $\Lambda(R,\boldsymbol{\varrho}) = \int_{t_1}^{t_2} \mathrm{d}t \left| \int \mathrm{d}t'\, \Phi(t-t')\, I(t', \boldsymbol{R}; \hat{\boldsymbol{s}}(\boldsymbol{\varrho})) \right|$
- RTE solved by partial wave expansion,

$$I(t,R;\hat{\boldsymbol{s}}(\theta)) \equiv I(t,R;\theta) = \sum_l \mathrm{P}_l(\cos\theta)\; I_l(t,R)$$

$$\Lambda_l(R) = \int_{t_1}^{t_2} \mathrm{d}t \left| \int \mathrm{d}t'\, \Phi(t-t')\, I_l(t',R) \right|$$

*Fourier-Legendre series, large no of terms*

$$\Lambda(R,\varrho) = \Lambda(R,\theta) = \sum_l \mathrm{P}_l(\cos\theta)\, \Lambda_l(R)$$

*Hankel transform fine sampling in* $\boldsymbol{\theta}$

$$\widetilde{\Lambda}(R,q) = \frac{1}{2\pi} \int \mathrm{d}\varrho\, \varrho\, \mathrm{J}_0(q\varrho)\, \Lambda(R,\varrho)$$

*a short-cut*
*- large no of terms*
*- no need for sampling in* $\boldsymbol{\theta}$

$$\widetilde{\Lambda}(R,q) = \sum_l D_l(q)\, \Lambda_l(R)$$

*modulation transfer function*

*challenges:*
*- evaluation of Fourier transform by summing a very large number of P contributions (>10,000)*
*- fine sampling in time (~1000 points)*

- *the computed MTF*

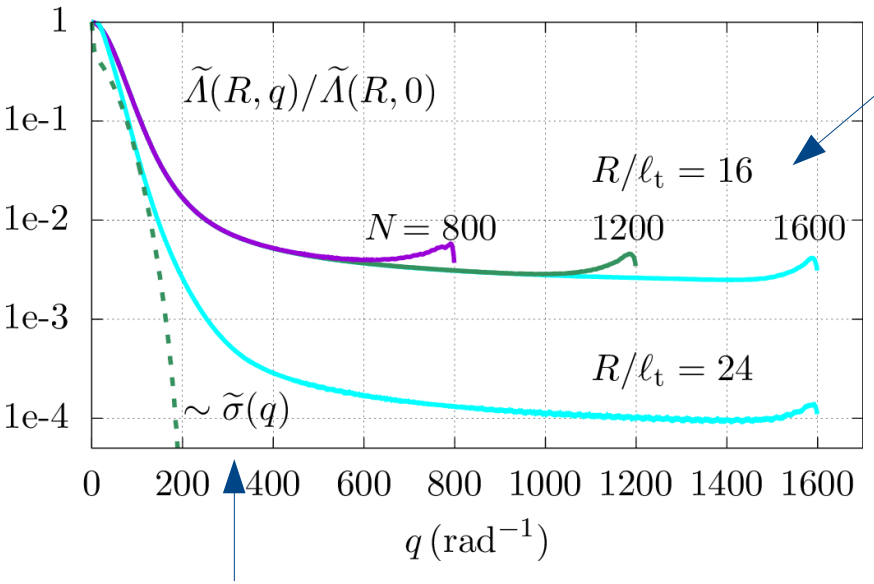


*good convergence with truncation* $N \to \infty$

*for comparison: Hankel transform of the cross-section*

## properties of PSF and MTF

PSF

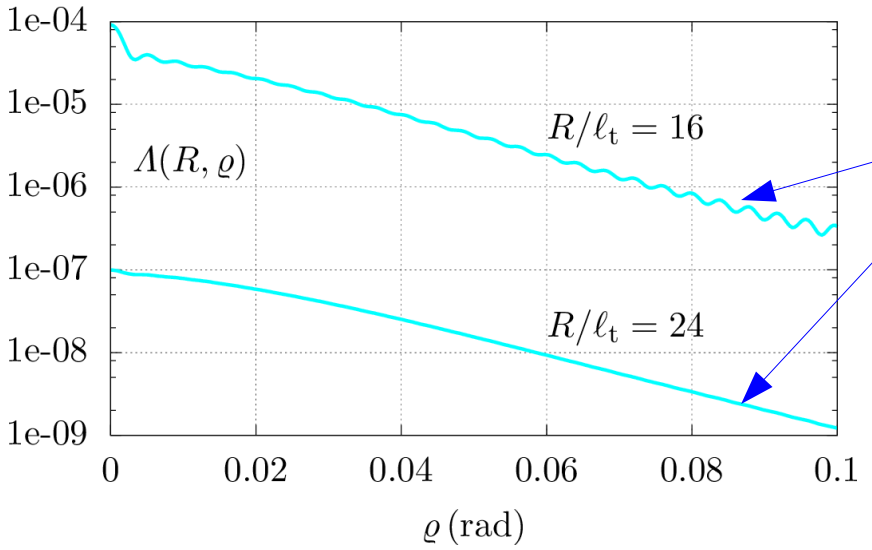


*wide angular ($\varrho$) distribution due to low level of large q's*

*image blurring*

MTF

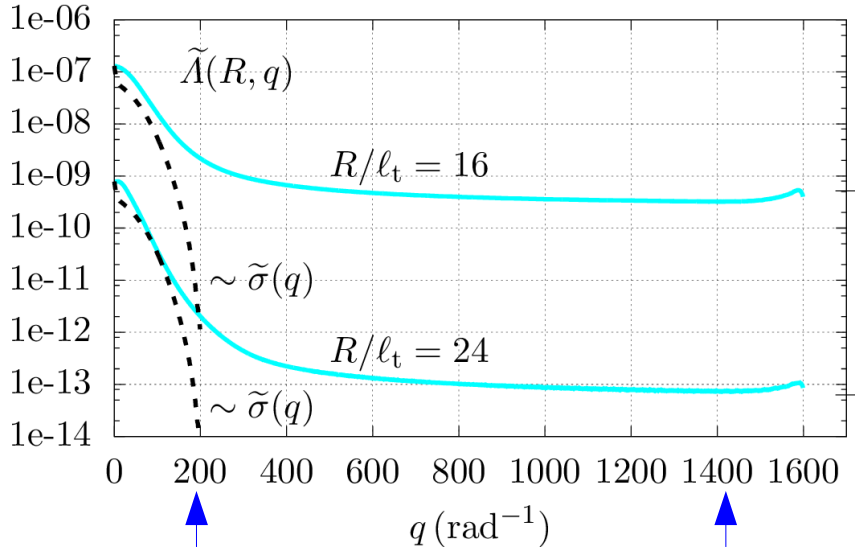


$e^{-0.64\cdot(24-16)} \approx 6.0 \cdot 10^{-3}$

*(reduced attenuation of small q component)*

$e^{-(24-16)} \approx 3.4 \cdot 10^{-4}$

*(strong attenuation of large q component)*

*small q's generate a wide component of PSF but decay slowly with distance*

*large q's generate a narrow component of PSF but decay with distance as a coherent contribution*

*devise a strategy to slow the decay of MTF with increasing q*

- *one of the approaches to reduce blurring: regularized deconvolution*

*(enhancing large spatial frequencies in the MTF)*

$$\widetilde{F}(\boldsymbol{q}) = \widetilde{\Lambda}(\boldsymbol{q})\,\widetilde{f}(\boldsymbol{q}) + \widetilde{\eta}(\boldsymbol{q})$$

*blurred image* — $\widetilde{F}(\boldsymbol{q})$; *MTF* — $\widetilde{\Lambda}(\boldsymbol{q})$; *ideal image* — $\widetilde{f}(\boldsymbol{q})$; *noise* — $\widetilde{\eta}(\boldsymbol{q})$

*(note: we suppressed dependences on the distance R)*

*the purpose of deblurring:*

*reconstruct* $\widetilde{f}(\boldsymbol{q})$ *from the observed image* $\widetilde{F}(\boldsymbol{q})$ *and the known MTF* $\widetilde{\Lambda}(\boldsymbol{q})$ *by solving the equation*

$$\widetilde{\Lambda}(\boldsymbol{q})\,\widetilde{f}(\boldsymbol{q}) = \widetilde{F}(\boldsymbol{q}) - \widetilde{\eta}(\boldsymbol{q})$$

$$\widetilde{f}(\eta;\boldsymbol{q}) = \frac{\widetilde{F}(\boldsymbol{q})}{\widetilde{\Lambda}(\boldsymbol{q})} - \frac{\widetilde{\eta}(\boldsymbol{q})}{\widetilde{\Lambda}(\boldsymbol{q})}$$

*but this is usually an ill-conditioned inverse problem (*$\widetilde{\Lambda}(\boldsymbol{q})$ *is, typically, small for large* $\boldsymbol{q}$ *) and the r.h.s. is not known exactly (noise)*

## regularized deconvolution

- *naïve inverse filtering:*

$$\widetilde{f}(\eta;\boldsymbol{q}) = \frac{\widetilde{F}(\boldsymbol{q})}{\widetilde{\Lambda}(\boldsymbol{q})} - \frac{\widetilde{\eta}(\boldsymbol{q})}{\widetilde{\Lambda}(\boldsymbol{q})}$$

*results in potentially (and typically) large noise contribution*

*the reason: typically, both* $\widetilde{F}(\boldsymbol{q})$ *and* $\widetilde{\Lambda}(\boldsymbol{q})$ *rapidly decay for large* $|\boldsymbol{q}|$*,*
*but* $\widetilde{\eta}(\boldsymbol{q})$ *may remain constant*

*this happens for white noise: noise at different pixels is uncorrelated, hence noise fluctuations have a very wide spectrum:* $\widetilde{\eta}(\boldsymbol{q}) \to \eta_0 > 0$ *for* $|\boldsymbol{q}| \to \infty$

- *one of solutions: regularized deconvolution (Tikhonov and related methods) balancing error due to regularization against reduced noise*

$$\widetilde{f}_\beta(\eta;\boldsymbol{q}) = \frac{\widetilde{\Lambda}(\boldsymbol{q})\,\widetilde{F}(\boldsymbol{q})}{\widetilde{\Lambda}^2(\boldsymbol{q}) + \beta^2} - \frac{\widetilde{\Lambda}(\boldsymbol{q})\,\widetilde{\eta}(\boldsymbol{q})}{\widetilde{\Lambda}^2(\boldsymbol{q}) + \beta^2}$$

*- the term* $\beta^2$ *is negligible when* $\widetilde{\Lambda}(\boldsymbol{q})$ *is large*
*and prevents indefinite growth of the noise term when* $\widetilde{\Lambda}(\boldsymbol{q})$ *is small*
*- the parameter* $\beta$ *can be adjusted so that the noise term in* $f_\beta(\eta;\boldsymbol{q})$
*is either smaller than the signal or both are negligible*

## *regularized deconvolution*

*to assess the improvement in resolution,*

*- we apply deblurring to the PSF itself,* $F \rightsquigarrow \Lambda$ *, hence*

$$\widetilde{f}_\beta(\eta;\boldsymbol{q}) = \frac{\widetilde{\Lambda}(\boldsymbol{q})\left[\widetilde{F}(\boldsymbol{q}) - \eta(\boldsymbol{q})\right]}{\widetilde{\Lambda}^2(\boldsymbol{q}) + \beta^2} \quad \rightsquigarrow \quad \frac{\widetilde{\Lambda}(\boldsymbol{q})\left[\widetilde{\Lambda}(\boldsymbol{q}) - \eta(\boldsymbol{q})\right]}{\widetilde{\Lambda}^2(\boldsymbol{q}) + \beta^2}$$

*- we normalize* $\widetilde{\Lambda}$ *to* $\widetilde{M}(\boldsymbol{q}) = \dfrac{\widetilde{\Lambda}(\boldsymbol{q})}{\widetilde{\Lambda}(\boldsymbol{0})}$ *and redefine* $\widetilde{\eta}(\boldsymbol{q})$ *and* $\beta$*, hence*

$$\widetilde{f}_\beta(\eta;\boldsymbol{q}) \quad \rightsquigarrow \quad \frac{\widetilde{M}(\boldsymbol{q})\left[\widetilde{M}(\boldsymbol{q}) - \eta(\boldsymbol{q})/\widetilde{\Lambda}(\boldsymbol{0})\right]}{\widetilde{M}^2(\boldsymbol{q}) + \beta^2/\widetilde{\Lambda}^2(\boldsymbol{0})} \quad \rightsquigarrow \quad \frac{\widetilde{M}(\boldsymbol{q})\left[\widetilde{M}(\boldsymbol{q}) - \eta(\boldsymbol{q})\right]}{\widetilde{M}^2(\boldsymbol{q}) + \beta^2} \equiv \widetilde{M}_\beta(\eta,\boldsymbol{q})$$

*where new* $\widetilde{\eta}(\boldsymbol{q})$ *and* $\beta$ *are normalized relative to* $\widetilde{\Lambda}(\boldsymbol{0})$

$\widetilde{M}_\beta(\boldsymbol{q}) \equiv \widetilde{M}_\beta(0;\boldsymbol{q})$ *is expected to have a wider* $\boldsymbol{q}$ *distribution than* $\widetilde{M}(\boldsymbol{q})$*,*

*hence, the inverse Fourier transform* $\Lambda_\beta(\boldsymbol{\varrho}) = \displaystyle\int \frac{\mathrm{d}^2 q}{(2\pi)^2}\, \mathrm{e}^{\,\mathrm{i}\,\boldsymbol{q}\cdot\boldsymbol{\varrho}}\, \widetilde{M}_\beta(\boldsymbol{q})$
*should be narrower than* $\Lambda(\boldsymbol{\varrho})$

► *enhancing large spatial frequencies in the MTF*

*- suppose* $\widetilde{\eta}(\boldsymbol{q})$ *is white noise,* $\widetilde{\eta}(\boldsymbol{q}) \approx \eta_0 > 0$, *assume* $\eta_0 \ll 1$

*- choose* $\beta$ *such that* $\eta_0 \ll \beta \ll 1$

$$\widetilde{f}_\beta(\eta;\boldsymbol{q}) = \frac{\widetilde{M}(\boldsymbol{q})\left[\widetilde{M}(\boldsymbol{q}) - \eta_0\right]}{\widetilde{M}^2(\boldsymbol{q}) + \beta^2} \equiv S(q) + N(q)$$

*- then we can show that noise contribution is small*

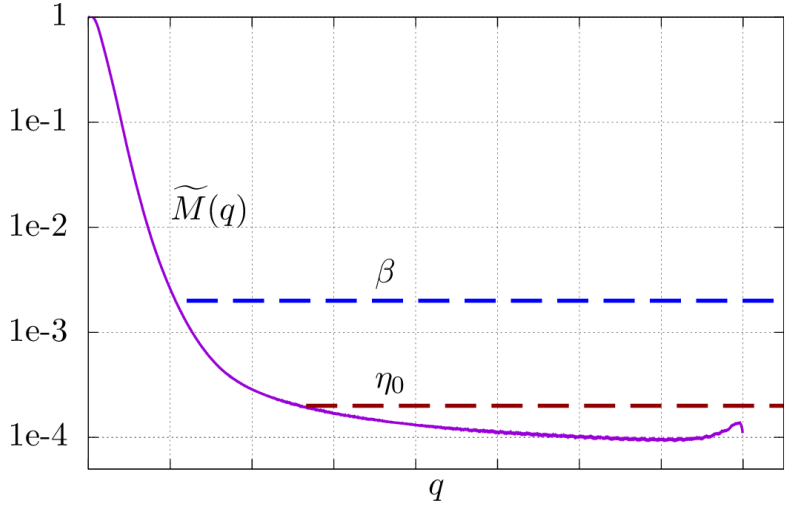


*the region* $\beta \ll \widetilde{M}(q) \le 1$

$$S(q) \approx 1$$

$$\frac{|N(q)|}{S(q)} \approx \frac{\eta_0}{\widetilde{M}(q)} \ll 1$$

*the region* $\eta_0 \ll \widetilde{M}(q) \ll \beta$

$$S(q) \approx \frac{\widetilde{M}^2(q)}{\beta^2} \ll 1$$

$$\frac{|N(q)|}{S(q)} \approx \frac{\eta_0}{\widetilde{M}(q)} \ll 1$$

*noise small relative to signal*

*the region* $0 < \widetilde{M}(q) < \eta_0 \ll \beta$

$$\frac{|N(q)|}{S(q)} \approx \frac{\eta_0}{\widetilde{M}(q)} > 1$$

*noise may be larger than signal*

$$S(q) \approx \frac{\widetilde{M}^2(q)}{\beta^2} \lll 1$$

$$|N(q)| \approx \frac{\widetilde{M}(q)\,\eta_0}{\beta^2} < \frac{\eta_0^2}{\beta^2} \lll 1$$

***but***

*both signal and noise are very small*

## regularized deconvolution

- *MTFs and PSFs in original and deblurred images*

*Note: the regularization parameter $\beta$ is chosen above the level of the "large q component" i.e., the "large q component" may be below the noise level*

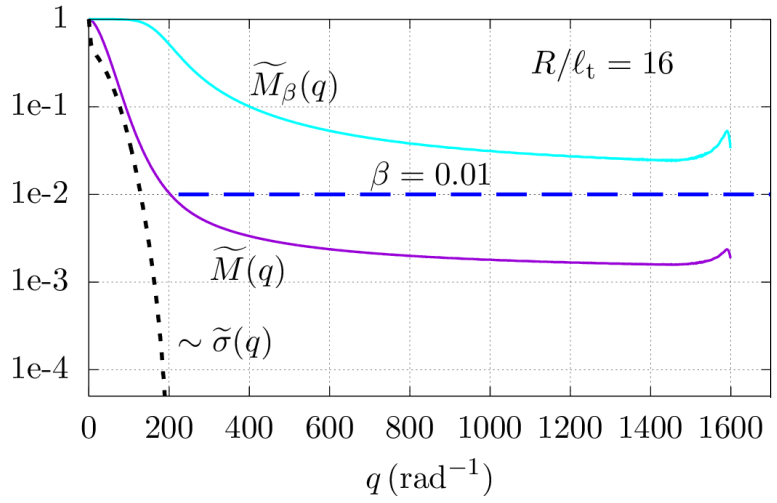


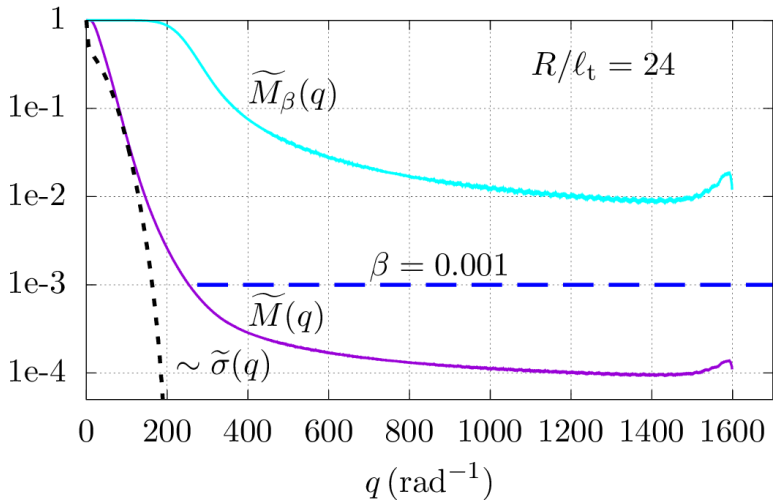


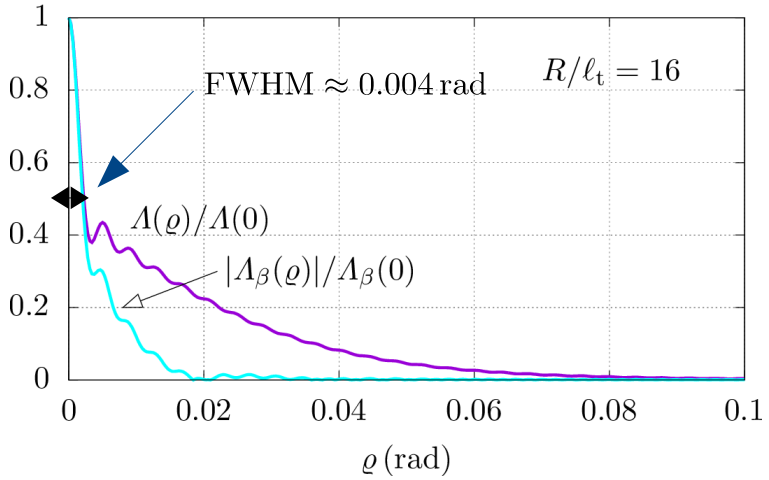


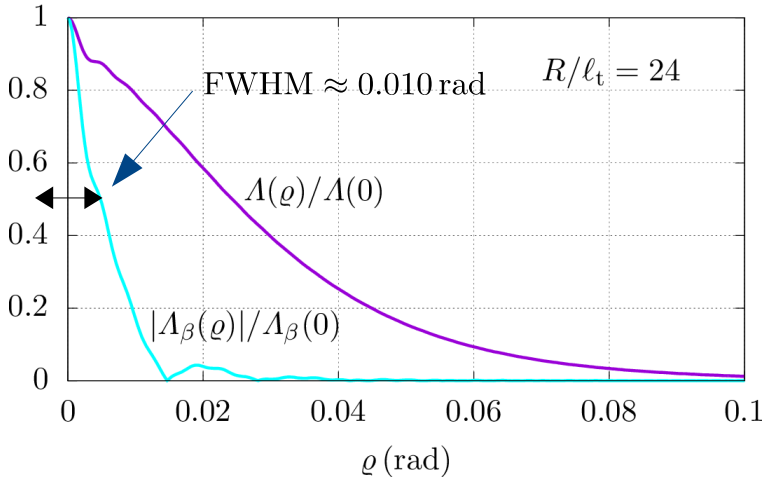

- *MTFs and PSFs in original and deblurred images*

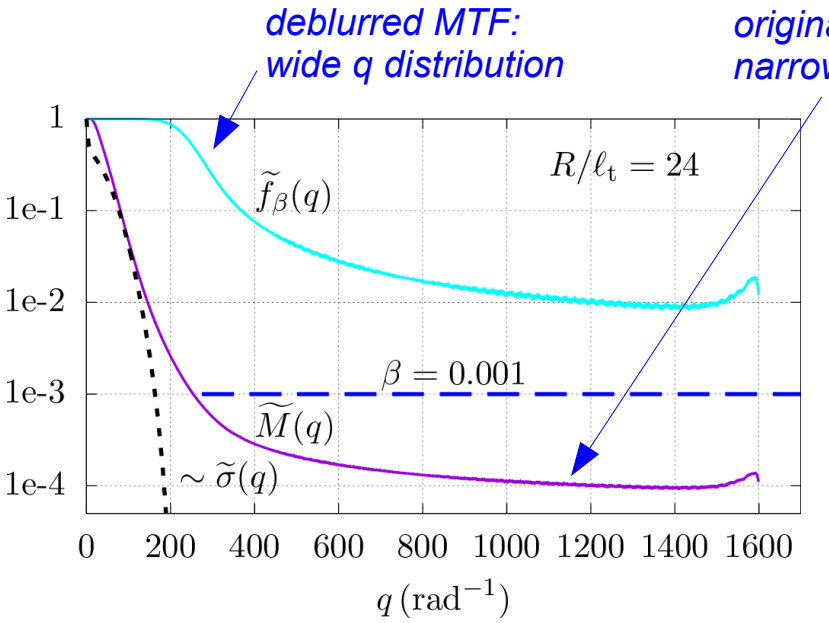


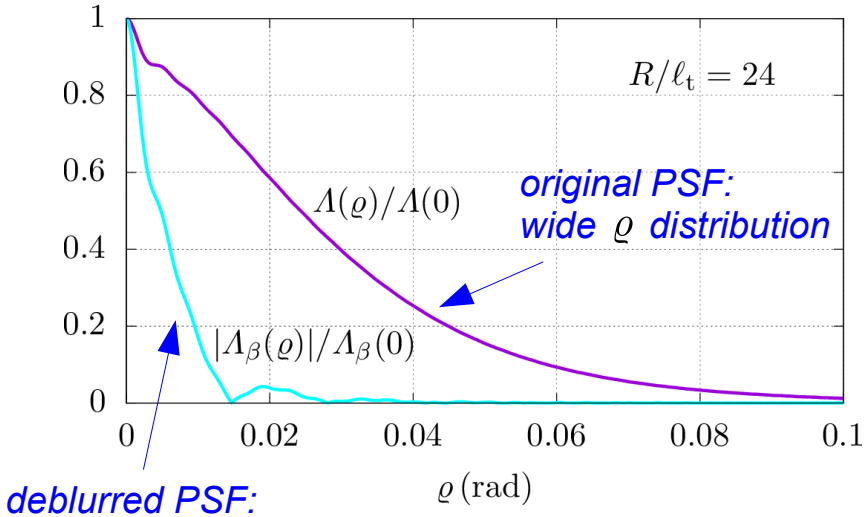


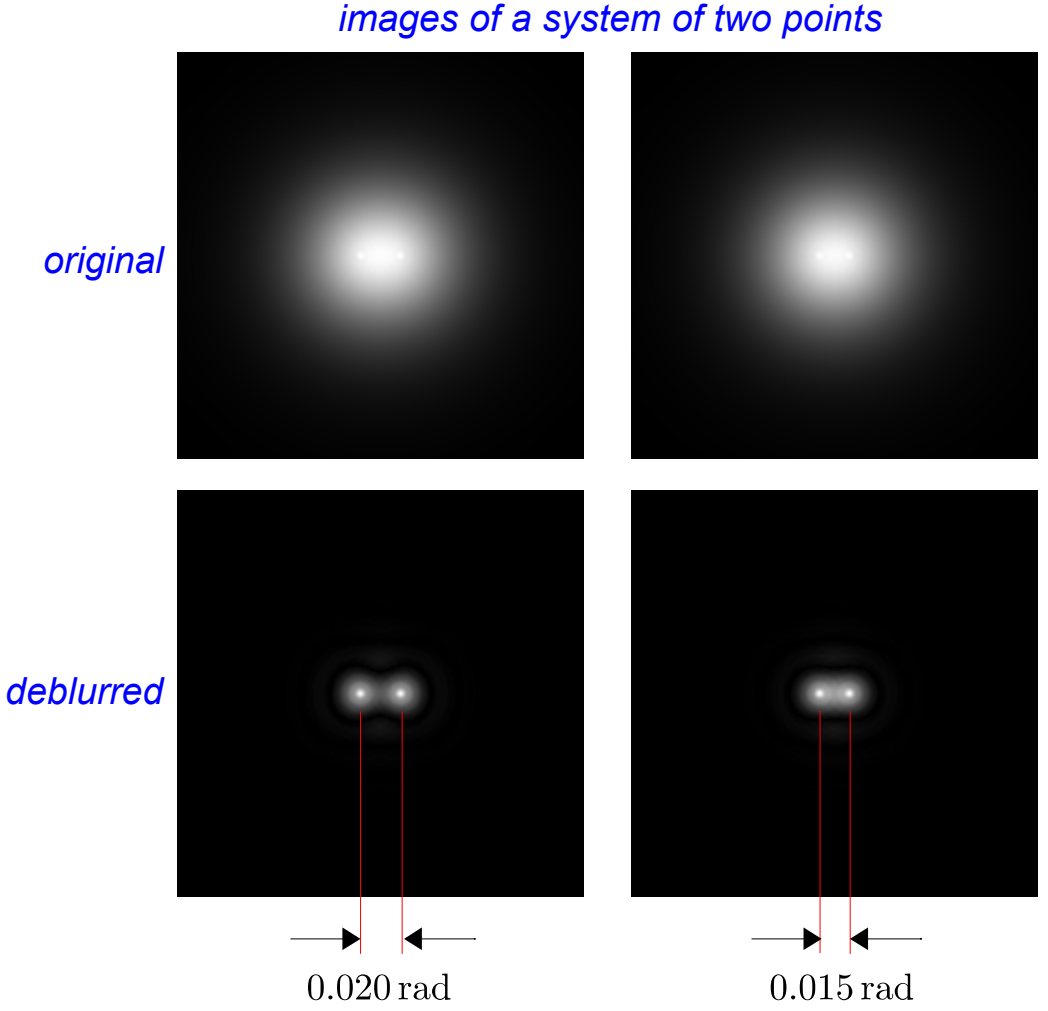

## summary

*we extended our work on early time diffusion phenomenon*

- *we identified RTE modes responsible for early and late time diffusion*
- *we achieved enhancement of the early time diffusion component by matching the source angular flux distribution to that of dominant RTE propagation modes responsible for early time diffusion*
- *we evaluated point spread function (PSF) and modulation transfer function (MTF) of RTE for medium consisting of large (wrt pulse carrie wavelength) scatterers*
- *we discussed imaging scenario involving early time diffusion signal and regularized deconvolution (utilizing modulation transfer function and Tikhonov regularizarion)*

*regularized deconvolution led to improved image angular resolution*

■ *estimates of angular and z-resolution in propagation through a slab of random medium*

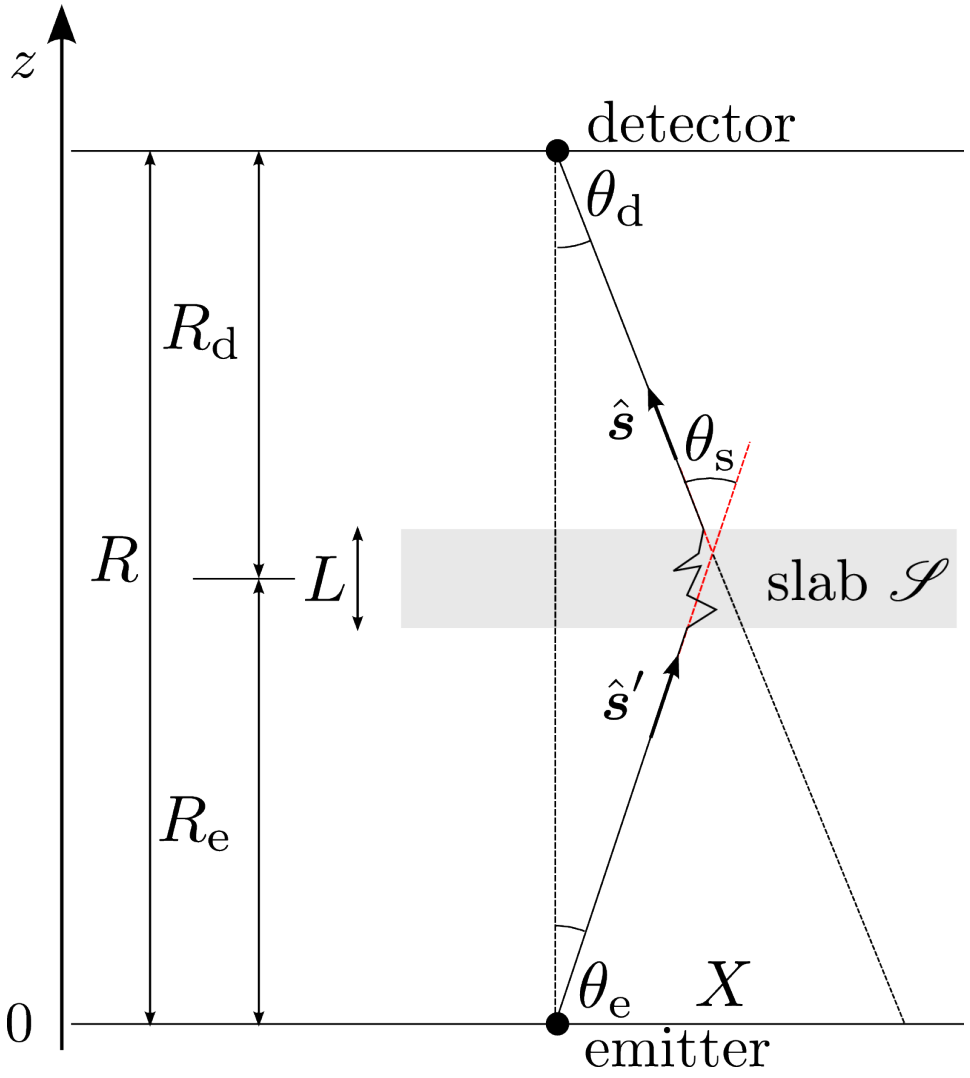


▶ *angular resolution*

$$\Theta \approx \frac{R_{\rm e}}{R}\,\theta_{\rm s}$$

*the corresponding transverse spatial resolution*

$$X \approx R_{\rm e}\,\theta_{\rm s}$$

*in analogy to shower-curtain effect. resolution attains min when slab is located close to emitter*

▶ *range resolution (path-length excess)*

$$Z \approx \left(2\,\frac{R_{\rm e}\,R_{\rm d}}{R} + L\right)\frac{L\,\theta_0^2}{4\,\ell}$$

- *estimates of angular and z-resolution in propagation through a slab of random medium*

  - *by extracting ETD signal we obtain a very good range resolution*

  - *the angular resolution would be*

    *- very good in most laboratory-scale imaging problems (including biomedical applications)*

    *- fairly good in short/medium-range (~ 100 m) atmospheric imaging*

    *- would deteriorate in long-range (kilometers) atmospheric imaging*

*THANK YOU !*

## enhancing early-time diffusion by adjusting the source

- *intensity* (radiance integrated over received flux directions $\hat{\boldsymbol{s}}$) is a convolution of the *Green function* with the *radiance source*

$$I(t,\boldsymbol{R}) = \int \mathrm{d}^2\hat{s} \int \mathrm{d}t' \mathrm{d}^3R' \mathrm{d}^2\hat{s}' \; \Gamma(t-t', \boldsymbol{R}-\boldsymbol{R}'; \hat{\boldsymbol{s}}, \hat{\boldsymbol{s}}') \; S(t', \boldsymbol{R}'; \hat{\boldsymbol{s}}')$$

- *substitute expression of the Green function in terms of its eigenmodes*

$$I(t,\boldsymbol{R}) = v_0 \sum_j \int \frac{\mathrm{d}^3P}{(2\pi)^3} \int \mathrm{d}^2\hat{s} \; \Psi^0_{j,\boldsymbol{P}}(t,\boldsymbol{R},\hat{\boldsymbol{s}}) \int \mathrm{d}^2\hat{s}' \int_{-\infty}^{t} \mathrm{d}t' \mathrm{d}^3R' \, \Psi^{0\,\mathsf{C}}_{j,\boldsymbol{P}}(t', \boldsymbol{R}', \hat{\boldsymbol{s}}'(\theta,\phi)) S(t'; \boldsymbol{R}'; \hat{\boldsymbol{s}}')$$

- *assume point-like source, located in the origin, and radiating in the z-direction with axially symmetric flux distribution*

$$S(t', \boldsymbol{R}'; \hat{\boldsymbol{s}}'(\theta,\phi)) = \delta^3(\boldsymbol{R}') \, S(t'; \hat{\boldsymbol{z}} \cdot \hat{\boldsymbol{s}}')$$

*normalization factor* (unit total energy)

$$S(t'; \hat{\boldsymbol{z}} \cdot \hat{\boldsymbol{s}}') = S_0 \, \mathrm{e}^{-t'^2/2\,T_\mathrm{P}^2} \, \mathrm{e}^{-\theta^2/2\,\Theta^2}$$

- *evaluate intensity for several angular widths of the source*

$$\Theta_\sigma \approx 0.02\,\mathrm{rad} \qquad \Theta_\sigma \approx 0.05\,\mathrm{rad} \qquad \Theta_\sigma = \pi\,\mathrm{rad} \quad \text{(omnidirectional source)}$$

$$\Theta_\sigma \approx 0.021\,\mathrm{rad} \quad \text{(angular width of the scattering cross-section)}$$

## *example: model of a source*

- *a spatially small source emitting axially symmetric radiation in the z-axis direction with the $\hat{s}'$ angular distribution*

$$\sim \mathrm{e}^{-\theta'^{\,2}/2\,\Theta^2}$$

*and with the width in $\Theta$ of the order of the scattering cross-section*

$$\Theta_\sigma \approx 0.02\,\mathrm{rad}$$

- *observation point on the z axis at a large distance R, radiance integrated over flux arrival directions $\hat{s}$*